Transalveolar Osmotic and Diffusional Water Permeability in Intact Mouse Lung Measured by a Novel Surface Fluorescence Method

ETHAN P. CARTER, MICHAEL A. MATTHAY, JAVIER FARINAS, and A.S. VERKMAN

From the Departments of Medicine and Physiology, Cardiovascular Research Institute, University of California, San Francisco, San Francisco, California 94143

ABSTRACT A surface fluorescence method was developed to measure transalveolar transport of water, protons, and solutes in intact perfused lungs. Lungs from c57 mice were removed and perfused via the pulmonary artery (~2 ml/min). The airspace was filled via the trachea with physiological saline containing a membrane-impermeant fluorescent indicator (FITC-dextran or aminonapthalene trisulfonic acid, ANTS). Because fluorescence is detected only near the lung surface due to light absorption by lung tissue, the surface fluorescence signal is directly proportional to indicator concentration. Confocal microscopy confirmed that the fluorescence signal arises from fluorophores in alveoli just beneath the pleural surface. Osmotic water permeability (P_f) was measured from the time course of intraalveolar FITC-dextran fluorescence in response to changes in perfusate osmolality. Transalveolar P_f was 0.017 ± 0.001 cm/s at 23°C, independent of the solute used to induce osmosis (sucrose, NaCl, urea), independent of osmotic gradient size and direction, weakly temperature dependent (Arrhenius activation energy 5.3 kcal/mol) and inhibited by $HgCl_2$. P_f was not affected by cAMP activation but was decreased by 43% in lung exposed to hyperoxia for 5 d. Diffusional water permeability (P_d) and P_f were measured in the same lung from intraalveolar ANTS fluorescence, which increased by 1.8-fold upon addition of 50% D_2O to the perfusate. P_d was 1.3×10^{-5} cm/s at 23°C. Transalveolar proton transport was measured from FITC-dextran fluorescence upon switching perfusate pH between 7.4 and 5.6; alveolar pH half-equilibrated in 1.9 and 1.0 min without and with HCO_3^-, respectively. These results indicate high transalveolar water permeability in mouse lung, implicating the involvement of molecular water channels, and establish a quantitative surface fluorescence method to measure water and solute permeabilities in intact lung. Key words: alveolus • osmosis • fluorescent indicator • aquaporin • water channel

INTRODUCTION

There is continuous movement of water, ions, and small solutes between the airspace and blood compartments in the intact lung. Large quantities of fluid move out of the airspaces in the perinatal period, and there is net water movement into the airspaces in the normal adult lung to offset evaporative losses (Boucher, 1994; Olver, 1994). Water and solute transport also play a role in clinically important pathological conditions, including the formation and resolution of alveolar edema (Saumon and Basset, 1993; Matthay et al., 1996) and the correction of alveolar fluid composition after aspiration of acid, salt water, or fresh water. The major barrier between the airspace and blood compartments is the alveolar epithelium, which is in series with the relatively leaky capillary endothelium. In addition, although they comprise much less total surface area (Weibel, 1989), small and large airways also contain a fluid-transporting epithelial cell layer (Folkesson et al., 1996).

Address correspondence to Alan S. Verkman, M.D., Ph.D., Cardiovascular Research Institute, 1246 Health Sciences East Tower, Box 0521, University of California, San Francisco, San Francisco, CA 94143-0521. Fax: 415-665-3847; E-mail: verkman@itsa.ucsf.edu

The conventional approach to study transalveolar transport of salt and water is to flood the airspaces with fluids of specified osmolality and composition and to assay the composition of serially sampled airspace and/or blood compartment fluids (Basset et al., 1987; Goodman et al., 1987; Effros et al., 1989; Matthay et al., 1996). Various in situ and ex vivo lung preparations have been established for these studies. In the in situ perfused sheep lung, Folkesson et al. (1994*b*) showed that osmotic equilibration of hyperosmolar (900 mOsm) fluid instilled into the airspaces was rapid and inhibited reversibly by $HgCl_2$. Similar experiments have been performed to measure alveolar fluid composition in response to instillation of acids (Folkesson et al., 1995), fresh water (Acevedo and Robin, 1972), and hypertonic saline (Folkesson et al., 1994*a*). Significant limitations of this "instill and sample" approach include low time resolution, uncertainties in the sampling of true intraalveolar fluid, the need to use relatively large animals, and the technical difficulty and cost of the studies. The ability to measure transalveolar salt and water transport in mice is particularly important given the recent and anticipated development of transgenic knockout models for lung ion channels (e.g., CFTR) and water transporters.

J. GEN. PHYSIOL. © The Rockefeller University Press • 0022-1295/96/09/133/10 $2.00
Volume 108 September 1996 133–142

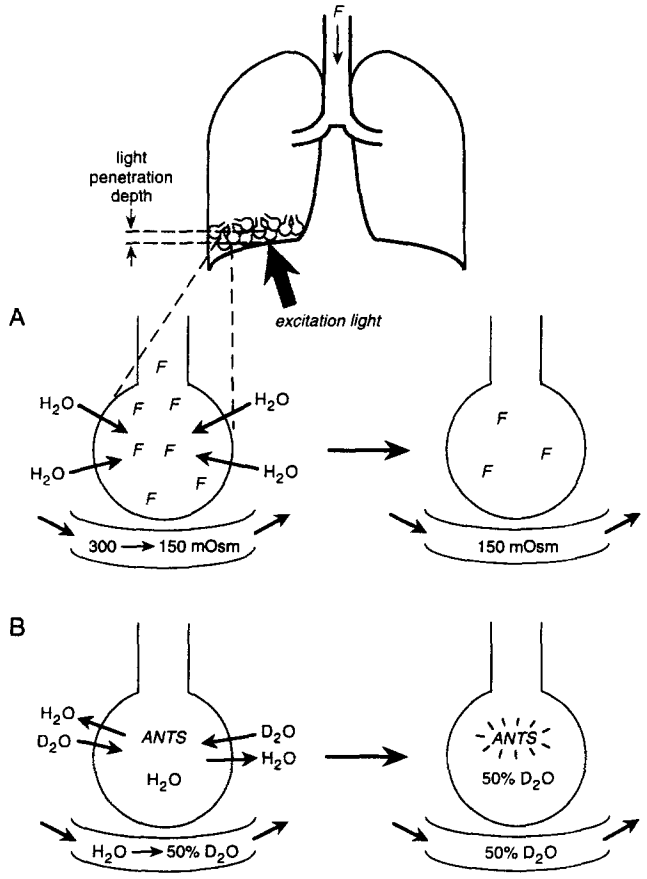

FIGURE 1. Strategy for measurement of osmotic and diffusional water permeability in the intact mouse lung. Illumination of the pleural surface results in excitation of fluorophores in the airspace only near the pleural surface ("light penetration depth"). (*A*) Osmotic water permeability (P_f) measured from the change in intraalveolar fluorophore concentration. In response to a change in perfusate osmolality from 300 to 150 mOsm, intraalveolar fluorophore is diluted. (*B*) Diffusional water permeability (P_d) measured from the increase in intraalveolar ANTS fluorescence in response to addition of 50% D_2O to the perfusate. See text for further explanations.

The purpose of this study was to develop and apply a new approach to measure continuously the composition of intraalveolar fluid in intact mouse lung. Our strategy was to fill the airspace of an isolated perfused mouse lung with physiological saline containing a membrane-impermeant fluorescent indicator. Fluorescent indicators and perfusion strategies were chosen to measure osmotic and diffusional water permeability in the same lung, and to follow the kinetics of intraalveolar pH in response to imposed transalveolar pH gradients. For measurement of osmotic water permeability (P_f),[1] the airspace was filled with a membrane-impermeant fluorophore at low concentrations in which there was no self-quenching or significant absorption of excitation light or emitted fluorescence (Fig. 1 *A*). Because of the finite penetration depth of excitation light, only lung tissue near the pleural surface is illuminated so that the surface fluorescence signal is proportional to the airspace fluorophore concentration. In response to an osmotic gradient, water will flow between the airspace and perfusate compartments, resulting in fluorophore concentration or dilution. Fluorophore concentration and thus osmolality is "sampled" by measurement of surface fluorescence. For determination of diffusional water permeability (P_d) (Fig. 1 *B*), the airspace is filled with physiological saline (in H_2O) containing the membrane-impermeant fluorophore aminonapthalene trisulfonic acid (ANTS), whose brightness (quantum yield) depends on solution H_2O vs. D_2O content (Kuwahara and Verkman, 1988). Upon switching the perfusate to an isosmolar solution containing D_2O, there is transalveolar exchange of H_2O for D_2O and an increase in surface fluorescence signal; P_d is determined from the time course of surface fluorescence, the relation between ANTS fluorescence vs. solution D_2O content, and alveolar surface-to-volume ratio. The method was applied to characterize in detail the water permeability properties of c57 mouse lung, and to measure the transport of urea and protons. Because high quality quantitative data can be obtained easily in small animals without the need to sample alveolar fluid, the fluorescence method established here should have numerous applications in lung transport physiology.

METHODS

Lung Preparation

c57 mice (Benton-Kingman, Freemont, CA; 20–25 g) were killed with intraperitoneal pentobarbital (150 mg/kg). The trachea was transected and cannulated in situ with polyethylene PE-50 tubing. The pulmonary artery and left atrium were transected, and the pulmonary artery was cannulated with PE-20 tubing. The cannulae were secured with 3-0 silk surgical thread. The heart and lungs were moved en bloc to a Lucite perfusion chamber for observation by epifluorescence microscopy (Fig. 2). One lung was positioned above a narrow channel (7 mm wide, 10 mm high, 33 mm long) in which HEPES-buffered Ringer's (HBR: 137 mM NaCl, 2.68 mM KCl, 1.25 mM $MgSO_4$, 1.82 mM $CaCl_2$, 5.5 mM glucose, 12 mM HEPES, 1.5% BSA, pH 7.4, 300 mOsm) was continuously perfused (10–20 ml/min) between the external pleural surface and the coverglass. The pulmonary artery was gravity perfused at constant pressure (25–35 cm H_2O) using a multi-solution reservoir and 4-way flow valve (vascular resistance 20–30 cm H_2O/mm per min). The pulmonary artery was initially perfused with HBR for 5 min to remove all blood and to set reservoir height for the desired perfusion rate (generally 1–2.5 ml/min). In some experiments, a membrane-impermeant fluorophore (FITC-dextran) was added to the perfusate solution. The temperature of the pulmonary artery and pleural surface perfusates were controlled by circulating water around the perfusion inflow tubing; effluent temperature was measured by a thermistor positioned near the outflow. The airspace was filled with 0.5–0.8 ml

[1] *Abbreviations used in this paper:* ANTS, aminonapthalene trisulfonic acid; P_d, diffusional water permeability; P_f, osmotic water permeability.

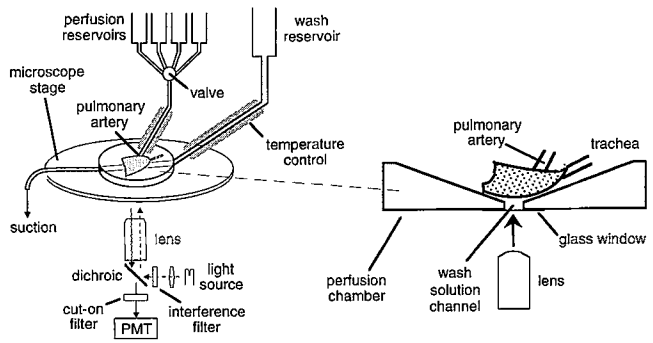

FIGURE 2. Instrumentation for measurement of pleural surface fluorescence in the ex vivo perfused mouse lung. Lungs and heart were positioned en bloc in a perfusion chamber on the stage of an inverted epifluorescence microscope. The trachea was cannulated for instillation of saline containing a fluorescent indicator. The pulmonary circulation was perfused via the pulmonary artery and the pleural surface was washed continuously with saline. Perfusate and wash effluent was withdrawn from the chamber by suction. Fluorescence was recorded from a 3–5 mm diameter spot on the lung surface. See text for details.

of HBR containing FITC-dextran (70 kD, 0.5–5 mg/ml; Sigma Chemical Co., St. Louis, MO) or aminonapthalene trisulfonic acid (ANTS, 5 mM, Molecular Probes Inc., Eugene, OR). Fluorescence measurements were carried out in a dark room. In some experiments, mice were exposed to 100% oxygen for 5 d to produce endothelial and mild epithelial lung damage (Frank et al., 1978; Crapo, 1986).

Pleural Surface Fluorescence Microscopy

The fluorescence intensity from a 3–5 mm diameter spot on the lung pleural surface was monitored using an inverted epifluorescence microscope (Nikon Diaphot) (Fig. 2). The spot was illuminated using a stabilized tungsten-halogen lamp (15 V, 5 amps) in series with a neutral density filter (optical density 1.0), interference filter, and dichroic mirror. A 10× dry objective (Leitz, numerical aperture 0.25) was used for all measurements. Emitted fluorescence was filtered by a cut-on filter and detected by a photomultiplier (R928S; Hamamatsu, Middlesex, NJ). Filter wavelength specifications were (interference, dichroic, cut-on): FITC-dextran (480 ± 5 nm, 510 nm, >515 nm); ANTS (380 ± 10 nm, 430 nm, >515 nm). The photomultiplier signal was amplified (Model 110; Ealing Corp., S. Natick, MA) and digitized by a 12-bit analog-to-digital converter interfaced to a PC computer. The signal was filtered by a single pole RC filter with a 0.3-s time constant. Data were acquired at 30 Hz, and 30 consecutive samplings were averaged for each displayed point. No photobleaching was observed with the low illumination intensity used here.

Osmotic Water Permeability

The airspace was filled with HBR (300 mOsm, measured by osmometer; Advanced Instruments, Needham Heights, MA) containing either FITC-dextran or ANTS, and the pulmonary artery was perfused with HBR for at least 5 min. An airspace-to-perfusate osmotic gradient was generated by switching the perfusate to HBR with added sucrose (hyperosmolar) or HBR diluted with distilled water (hypoosmolar). In some experiments NaCl or urea were used in place of sucrose. The time course of lung surface fluorescence was monitored continuously. A series of perfusate fluid exchanges and transport measurements could be done for >1 h without change in vascular resistance or water permeability.

Osmotically induced volume flux, J_v (cm^3/s), is defined by: $J_v = dV/dt = P_f S\, v_w \Delta C$, where P_f (cm/s) is the osmotic water permeability coefficient, S (cm^2) is surface area, v_w (18 cm^3/mol) is the partial molar volume of water, and ΔC is the difference in osmolality between perfusate and airspace fluids. Because the surface fluorescence signal, $F(t)$, is directly proportional to intraalveolar fluorophore concentration (see RESULTS) and thus to intraalveolar fluid osmolality, it follows that $F(t)V(t) = F_o V_o$, where F_o is initial fluorescence and V_o is initial airspace fluid volume. Differentiating, $dV/dt = -[F_o V_o / F(t)^2]\, dF(t)/dt$, and utilizing the J_v definition above: $d(F/F_o)/dt = -(F/F_o)^2 P_f v_w (S/V_o)\Delta C$. Evaluating $d(F/F_o)/dt$ at zero time (where $F = F_o$),

$$P_f = [d(F/F_o)/dt]_{t=0} / [(S/V_o) v_w \Delta C], \quad (1)$$

where $[d(F/F_o)/dt]_{t=0}$ is computed from the initial slope of a biexponential fit to the measured fluorescence time course, and surface-to-volume ratio, S/V_o (cm^{-1}), is determined from serial confocal micrographs of surface alveoli (see below). Eq. 1 assumes that osmolality is constant throughout the airspace compartment and that alveolar surface area constitutes the major contribution to total airspace surface area. Eq. 1 also assumes that osmotically active solutes have a unity reflection coefficient. In experiments in which higher airspace fluorophore concentrations were used, $F(t)$ is not directly proportional to fluorophore concentration because of inner filter effects (absorbance of light by fluorophores); the right side of Eq. 1 is then multiplied by $[C_p/C_{al} - 1]/[F_{final}/F_o - 1]$, where C_p/C_{al} is the ratio of perfusate to initial airspace fluid osmolality and F_{final} is final fluorescence.

Diffusional Water Permeability

The airspace was filled with HBR (in 100% H_2O) containing ANTS, a membrane-impermeant fluorophore whose quantum yield is insensitive to ionic strength and pH, but increases 3.2-fold when H_2O is replaced by D_2O (Kuwahara and Verkman, 1988). The pulmonary artery was initially perfused with HBR in 100% H_2O. The perfusate was then switched to isosmolar HBR prepared in 50% H_2O–50% D_2O. Diffusional exchange of D_2O with H_2O resulted in an increase in intraalveolar D_2O content and thus increased ANTS fluorescence.

Diffusional water permeability is defined by: $df_{D2O}/dt = P_d(S/V_o)\,\Delta f_{D2O}$, where f_{D2O} (0 to 1) is the fractional content of D_2O, and P_d (cm/s) is the diffusional water permeability coefficient. As determined by fluorimetry, f_{D2O} is related to relative ANTS fluorescence, F/F_o by: $f_{D2O} = -0.11(F/F_o)^2 + 0.91(F/F_o) - 0.79$ (Folkesson et al., 1996). Since $df_{D2O}/dt = [df_{D2O}/d(F/F_o)]\,[d(F/F_o)/dt)]$, P_d can be determined from df_{D2O}/dt at zero time, just after addition of 50% D_2O ($\Delta f_{D2O} = 0.5$) to the perfusate,

$$P_d = [d(F/F_o)/dt]_{t=0}\,[df_{D2O}/d(F/F_o)]_{F=Fo} / [0.5(S/V_o)], \quad (2)$$

where $[df_{D2O}/d(F/F_o)]_{F=Fo}$ is evaluated from the f_{D2O} vs. F/F_o relation above to be 0.69. To correct for a signal amplitude $[F_{final}/F_o - 1]$ that differs from that predicted by the in vitro f_{D2O} vs. F/F_o relation, the right hand term in Eq. 2 is multiplied by $1.81/[F_{final}/F_o - 1]$, where the factor 1.81 is the predicted increase in ANTS fluorescence in 50% D_2O relative to that in 100% H_2O.

In some experiments, P_f and P_d were measured in the same lung whose airspace contained ANTS. P_f was first measured from the time course of pleural surface fluorescence in response to a change in perfusate osmolality using a hyperosmolar perfusate in 100% H_2O. (In 100% H_2O, the ANTS signal is directly proportional to intraalveolar ANTS concentration.) After return of the perfusate to HBR (in 100% H_2O), P_d was measured as described

above by switching the perfusate to an isosmolar solution containing 50% D_2O.

Proton Transport Measurements

The airspace was filled with HBR containing 1 mg/ml FITC-dextran (pKa 6.4) for continuous measurement of intraalveolar pH. The perfusate consisted of HBR (titrated to pH 7.4 or 5.5) or HBR in which 25 mM Cl^- was replaced with HCO_3^-. Surface fluorescence intensity was converted to airspace fluid pH from an in vitro FITC-dextran titration.

Confocal Microscopy

Confocal microscopy was carried out to visualize the fluorophore distribution and to determine alveolar geometry. The airspace was filled with HBR containing FITC-dextran and the pulmonary artery was perfused as described above. The pleural surface was viewed using a Leitz upright epifluorescence microscope with coaxial-confocal attachment (Technical Instruments, San Francisco, CA). A coverglass (thickness 0.17 mm) was positioned over the lung surface by a rigid support for visualization of fluorescently stained alveoli with a 60× Plan-Apo objective (Nikon, oil immersion, numerical aperture 1.4). Images (512 × 512 pixels, 14-bit resolution) were acquired by a cooled CCD camera using PMIS software (Photometrics, Tuscon, AZ) (Zen et al., 1992). The instrument z-resolution for rejection of out-of-focus fluorescence was ~1 μm. Alveolar surface-to-volume ratio was computed from serial images acquired 4.5 μm apart using a three-dimensional image reconstruction procedure reported previously (Farinas et al., 1995).

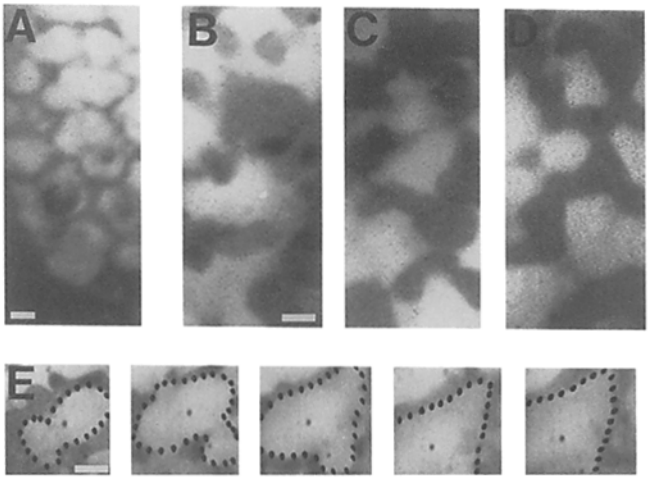

FIGURE 3. Confocal fluorescence microscopy of the pleural surface. The airspace was filled with HBR containing 1 mg/ml FITC-dextran. Confocal microscopy was done with a 25× dry or 60× oil immersion objective (see METHODS). (*A*) Low magnification confocal micrograph (25× objective) of pleural surface showing alveoli (*fluorescent round structures*) and a capillary vessel (*dark tubular structure, lower left*). Scale bar: 20 μm. (*B–D*) High magnification confocal micrographs (60×) with 300 mOsm perfusate (*B*) and 5 min after perfusion with 600 mOsm (*C*) or 150 mOsm (*D*) solutions. Scale bar: 10 μm. (*E*) Serial confocal micrographs taken at 4.5 μm z-intervals for reconstruction of alveolar geometry. Dots indicate boundary of an alveolus. Scale bar: 10 μm. See text for details.

RESULTS

Experiments were first carried out to verify the alveolar origin of the surface fluorescence signal and to show that the airspace fluorophore remains confined to the airspace compartment. Fig. 3 *A* shows a low magnification confocal micrograph of the lung surface after filling the airspace with physiological saline (HBR) containing FITC-dextran. Individual alveoli are seen with nonfluorescent septa separating alveoli, as well as a nonfluorescent blood vessel. At higher magnification, the geometry of individual alveoli are clearly visualized (Fig. 3 *B*). After changing perfusate osmolality to 600 mOsm or 150 mOsm, there was no obvious change in alveolar geometry as seen in representative confocal micrographs in Fig. 3, *C* and *D*. To examine quantitatively the effect of perfusate osmolality on alveolar geometry, the three-dimensional alveolar shape was reconstructed from serial confocal micrographs acquired at a series of z-positions (Fig. 3 *E*). The apparent alveolar size increased to a mean diameter of ~40 μm as the z-focus traversed individual alveoli. Well-resolved images could be obtained to ~25 μm beneath the lung surface because of light scattering by lung tissue. By image reconstruction (Farinas et al., 1995), alveolar surface-to-volume (S/V) ratio was computed to be 1,626 ± 107 cm^{-1} with the 300 mOsm perfusate, not significantly different from that of 1,533 ± 219 cm^{-1} with the 600 mOsm perfusate. These values are similar to the S/V of 1,500 cm^{-1} predicted for spherical alveoli of 40 μm diameter, as reported in morphological studies of mouse lung (Milsom, 1989). The S/V value is required for computation of absolute P_f and P_d (Eqs. 1 and 2). Measurements of perfusate effluent fluorescence indicated that <2% of airspace fluorophore appeared in the perfusate over 1 h. These studies indicate that the surface fluorescence signal arises from fluorophores confined to the airspace compartment.

Fig. 4 *A* shows the time course of lung surface fluorescence in response to changes in perfusate osmolality. In response to a sudden increase in perfusate osmolality to 600 mOsm, there was a prompt rise in fluorescence without a lag phase; final fluorescence was approximately twice the initial fluorescence. Perfusion with the original isosmolar solution returned the signal to baseline (without photobleaching). Final fluorescence decreased approximately twofold with the 150 mOsm perfusate. The quantitative agreement of the fluorescence signal change with perfusate osmolality indicates that surface fluorescence is a valid indicator of intraalveolar fluorophore concentration and that the fluorophore is confined to the airspace compartment (and not in the interstitium or vascular compartment). To estimate the effective penetration depth of the excitation light, the same experiment was performed at a higher concentration of FITC-dextran (5 mg/ml), where

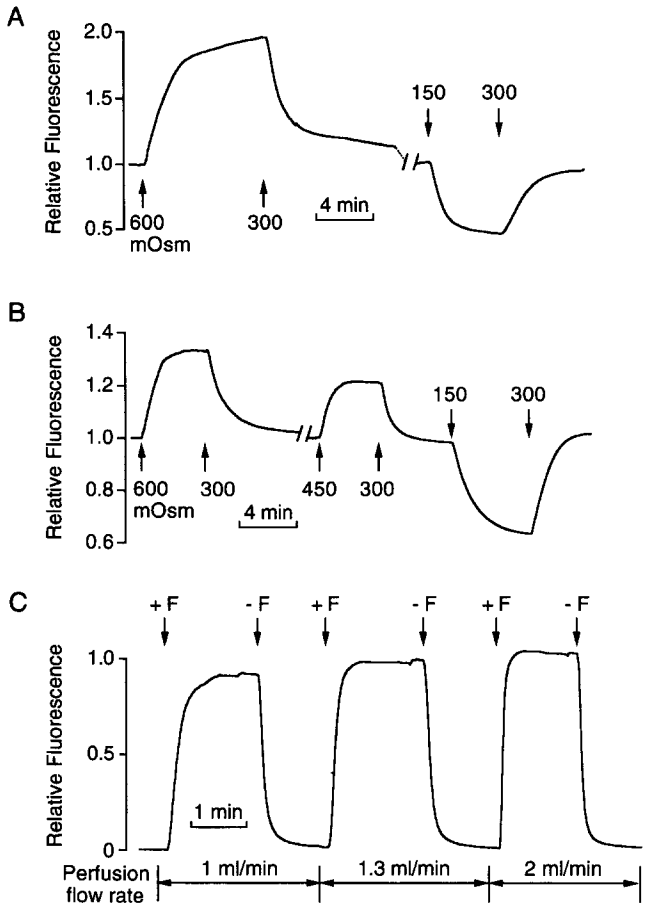

FIGURE 4. Measurement of osmotic water movement between airspace and capillary compartments in mouse lung. (*A* and *B*) Pleural surface fluorescence was recorded continuously in response to indicated changes in perfusate osmolality. The airspace was filled with HBR containing 0.5 mg/ml (*A*) or 5 mg/ml (*B*) FITC-dextran. (*C*) To measure perfusate exchange time, the airspace was filled with nonfluorescent HBR and the pulmonary artery was perfused at indicated flow rates with HBR containing 0 (*−F*) or 0.5 mM (*+F*) FITC-dextran.

significant absorption of excitation light (inner filter effect) should occur (Fig. 4 *B*). Although the curve shape was similar to that for the low FITC-dextran concentration (Fig. 4 *A*), the amplitude was much less than that predicted for a dilute fluorophore. Perfusion with the 600 mOsm solution gave a relative amplitude of 1.35 (2.0 predicted for dilute fluorophore); with the 150 mOsm perfusate, the amplitude was 0.65 (0.5 predicted). The attenuated signal amplitude results from a time-dependent change in lung light absorbance (sum of lung tissue and FITC absorbances) due to concentration or dilution of the intraalveolar FITC-dextran. Using these results and the measured optical density of FITC-dextran at 480 nm (0.18 for 5 mg/ml FITC-dextran, 1 mm pathlength), the effective light penetration depth is estimated to be ~300 μm for mouse lung in the absence of airspace fluorophore.

To compute P_f from the time course of surface fluorescence, the exchange of perfusion solutions must be fast compared to the kinetics of surface fluorescence change. Fig. 4 *C* shows the time course of lung surface fluorescence in response to addition and removal of FITC-dextran to the perfusate, where the airspace was filled with HEPES-buffer Ringer's (HBR) not containing fluorophore. The appearance and disappearance of fluorophore in the vascular space was very rapid (half-times of 12 s, 1 ml/min perfusate flow; 8.5 s, 1.25 ml/min; 4.5 s, 2 ml/min) and much faster than the half-times for osmotic equilibration in Fig. 4, *A* and *B* (half-times ~40 s). For a 600 mOsm perfusate, measured P_f values at 23°C were independent of perfusate flow rate (P_f = 0.016 cm/s, 1.36 ml/min; 0.015 cm/s, 1.67 ml/min; 0.017 cm/s, 2 ml/min), supporting the conclusion that measured P_f depends on the characteristics of the airspace-to-capillary barrier and is not limited by vascular flow rate. Further support for the adequacy of vascular perfusion was the lack of effect of papaverine (a vasodilator) on osmotically induced water flow (see Fig. 5 *E*). In addition, P_f was not dependent upon airspace pressure (0–5 cm H_2O) or the location of the illuminated spot on the lung surface (data not shown).

Osmotic water transport was further characterized in Fig. 5. Fig. 5 *A* shows that P_f for water movement between the airspace and perfusate compartments did not depend significantly on osmotic gradient size and direction. Average P_f was 0.017 ± 0.002 cm/s (SD, 23°C), a high value compared to most other biological membranes (see DISCUSSION), suggesting the involvement of molecular water channels. Fig. 5 *B* shows that osmotic water transport induced by equal osmotic gradients of sucrose, NaCl, and urea was similar (P_f = 0.017 ± 0.002 cm/s, sucrose; 0.018 ± 0.003, NaCl; 0.017 ± 0.001, urea), indicating that the reflection coefficients for NaCl and urea are near unity. In response to addition of 300 mM urea to the perfusate (final osmolality 600 mOsm), fluorescence increased promptly and remained elevated for >20 min (Fig. 5 *B*, *dashed curve*). This finding indicates very low permeability for urea movement between the airspace and capillary compartments. Fig. 5 *C* shows that P_f was weakly temperature dependent. An Arrhenius plot of ln P_f vs. reciprocal absolute temperature gave a slope (representing the activation energy, E_a) of 5.3 ± 1 kcal/mol. The low activation energy further supports the involvement of water channels (Verkman, 1989). Fig. 5 *D* shows that perfusate $HgCl_2$, a known inhibitor of water channels AQP-1 and AQP-5 (Preston et al., 1992; Van Hoek and Verkman, 1992; Raina et al., 1995), partially inhibits osmotic water movement in intact lung. Averaged P_f values are summarized in Fig. 5 *E*. P_f was decreased significantly by $HgCl_2$, but not by other known effectors of

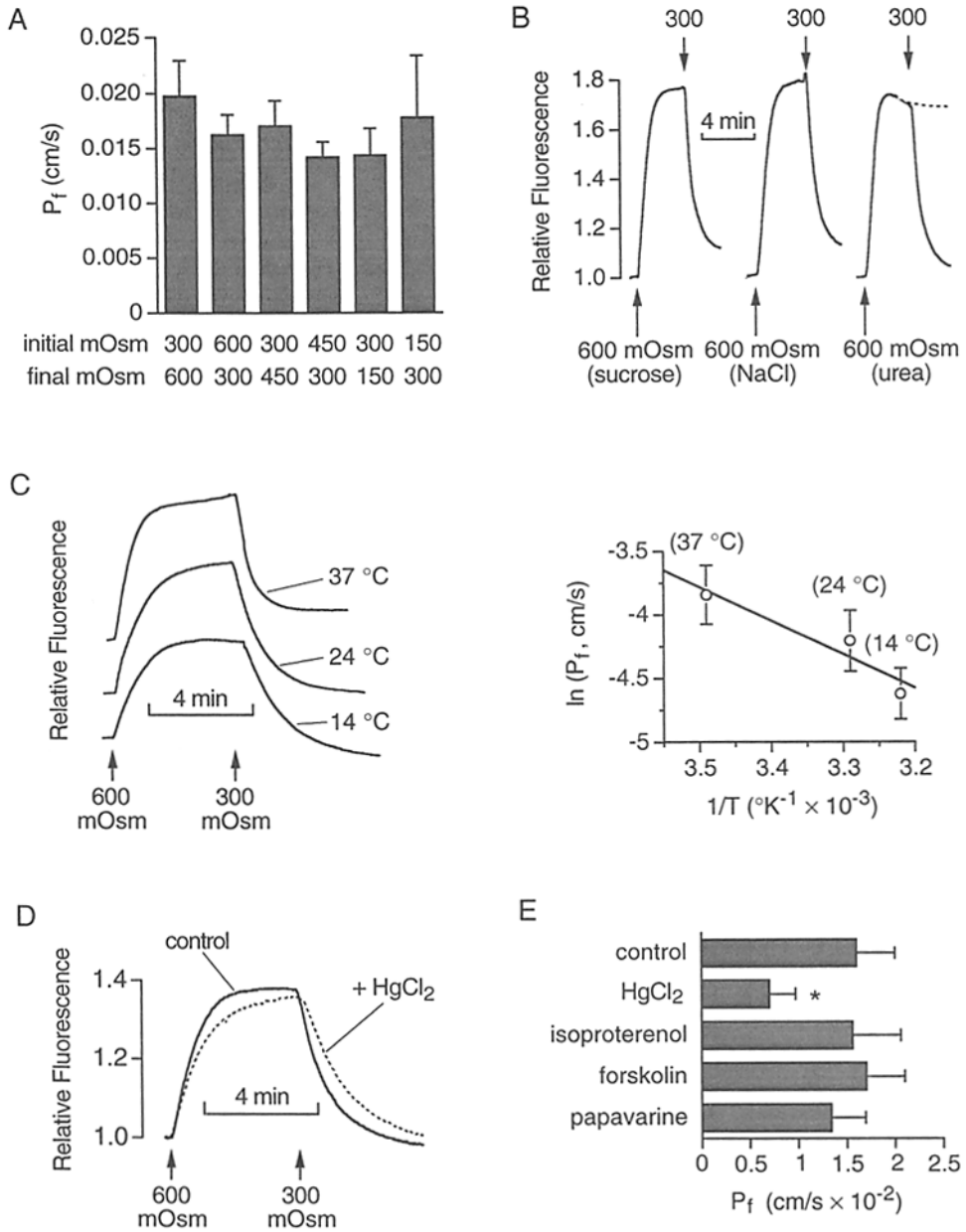

FIGURE 5. Properties of osmotic water permeability (P_f) in mouse lung. (*A*) P_f (mean ± SD, n = 4–5, 23°C) for indicated initial and final perfusate osmolalities. (*B*) Osmotic water movement induced by gradients of sucrose, NaCl, and urea. Indicated 600 mOsm solutions consisted of HBR containing 300 mOsm of added solute. (*C, left*) Representative surface fluorescence data for measurements performed at indicated temperatures. (*right*) Arrhenius plot for temperature dependence of P_f with slope (activation energy) of 5.3 kcal/mol (1 cal = 4.184 J). (*D*) Inhibition of osmotic water permeability by 0.1 mM $HgCl_2$ (added to perfusate, 14°C). (*E*) Summary of P_f values (SD, n = 4–10) measured in the presence of perfusate $HgCl_2$ (0.1 mM), isoproterenol (0.1 mM), forskolin (20 μM), or papaverine (0.1 mg/ml).

lung transport processes which act acutely, including isoproterenol and forskolin, or by the vasodilator papaverine.

To define further the properties of water transport in mouse lung, diffusional water permeability was measured. Fig. 6 *A* shows the time course of lung surface ANTS fluorescence in response to addition of 50% D_2O to the perfusate. There was a very rapid increase in fluorescence without a lag phase; fluorescence returned to the baseline value after perfusion with the original isosmolar H_2O buffer. The rate of fluorescence change increased with higher perfusion flow (from 1.7 to 2.0 ml/min), but did not change with a further increase in flow to 2.3 ml/min. The apparent half-time for the change in fluorescence at 1.8 ml/min perfusion (~33 s) was less than that in the P_f measurement (Fig. 4 *A*), yet slower than the perfusion exchange time (Fig. 4 *C*). Calculated P_d values at 23°C were 1.0×10^{-5} cm/s (1.7 ml/min perfusion flow), 1.5×10^{-5} cm/s (2.0 ml/min) and 1.6×10^{-5} cm/s (2.3 ml/min). These low P_d values indicate that diffusional water permeability is unstirred layer limited (see DISCUSSION). Fig. 6 *B* shows a measurement of P_f and P_d in the same lung in which the airspace was filled with physiological saline containing ANTS. In response to perfusion with hyperosmolar H_2O-containing buffer, ANTS fluorescence increased as a consequence of osmotic water movement. The fluorescence returned to the original level after perfusion

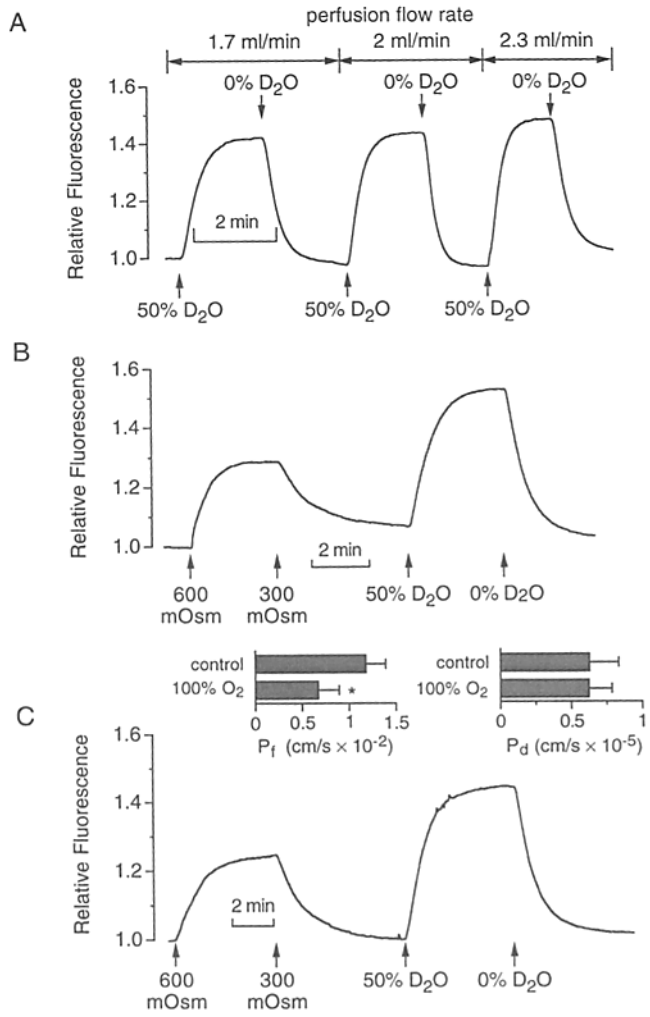

FIGURE 6. Measurement of osmotic and diffusional water permeability in the same lungs. The airspace was filled with HBR containing 2 mM ANTS, and the pulmonary artery was perfused at 23°C. (*A*) Time course of ANTS fluorescence in response to addition and removal of 50% D_2O to the isosmolar perfusate at indicated flow rates. (*B*) P_f was first measured from the change in ANTS fluorescence in response to indicated changes in perfusate osmolality in 100% H_2O solution. P_d was then measured as in *A*. (*C*) P_f and P_d measured in lungs from a mouse exposed to 100% O_2 for 5 d. (*Inset*) Averaged P_f and P_d values for control vs. hyperoxia-injured lungs (*difference significant at $P < 0.01$).

with the isosmolar H_2O solution. Subsequent perfusion with the isosmolar 50% D_2O solution gave increased fluorescence as a consequence of diffusional water movement. Averaged permeability values for four sets of measurements at 23°C were $P_f = 0.012 \pm 0.002$ cm/s and $P_d = (0.7 \pm 0.2) \times 10^{-5}$ cm/s.

Because P_d is unstirred layer limited and thus an indicator of vascular perfusion efficiency, measurement of P_f and P_d in the same lung is useful to evaluate the effect of lung injury on water transport. Fig. 6 *C* shows water permeability measurements on lungs from mice exposed to 100% oxygen for 5 d, which produces significant endothelial cell injury and some interstitial changes and epithelial cell damage (Frank et al., 1978; Crapo, 1986). In four mice (a fifth mouse was ill and not studied), averaged P_f decreased significantly by 43% (Fig. 6, *inset*), whereas P_d was unchanged. These results indicated that hyperoxia-induced lung injury is associated with decreased water permeability.

To demonstrate one other application of the surface fluorescence method, proton transport between the airspace and capillary compartments was measured. Fig. 7 shows the time course of intraalveolar pH, measured by FITC-fluorescence, in response to switching perfusate pH between 7.4 and 5.6 in the absence and presence of HCO_3^-. Upon switching perfusate pH to 5.6, there was a prompt decrease in surface fluorescence as intraalveolar pH decreased. The half-times for pH equilibration were ~1.9 min, which taken together with solution buffer capacity, gave an apparent proton permeability coefficient (P_{H+}, defined as in Verkman, 1987) of 0.06 cm/s. Alveolar pH returned to 7.4 promptly upon perfusion with the original solution, a finding with implications for the pathophysiology of acute acid aspiration (Folkesson et al., 1995). Upon addition of HCO_3^- to the perfusate, there was a transient decrease in alveolar pH corresponding to rapid perfusate-to-airspace movement of CO_2, followed by slower HCO_3^- movement and HCO_3^-/CO_2 equilibration. Subsequent perfusion with acidic and neutral buffers have pH equilibration half-times of ~1 min, suggesting the participation of a HCO_3^--dependent transporter.

DISCUSSION

The purpose of this study was to establish a surface fluorescence method to quantify water and solute permeability in intact lungs in order to characterize transalveolar water permeability in mouse lung. Our strategy was to fill the airspace compartment with physiological saline containing a membrane-impermeant fluorophore that functioned as an indicator of intraalveolar fluid composition. Intraalveolar osmolality and thus osmotic water permeability was inferred from indicator fluorescence intensity, exploiting the change in indicator concentration resulting from transalveolar water movement. Diffusional water permeability was measured using a fluorescent indicator having an H_2O-D_2O sensitive quantum yield. Transport of protons was measured using an intraalveolar pH indicator. Because nearly all of the fluorescence signal from the lung pleural surface originated from indicator in the intraalveolar compartment, the surface fluorescence signal provided an instantaneous and quantitative measure of intraalveolar fluid composition. Compared to previous approaches to measure transport between the alveolar and capillary

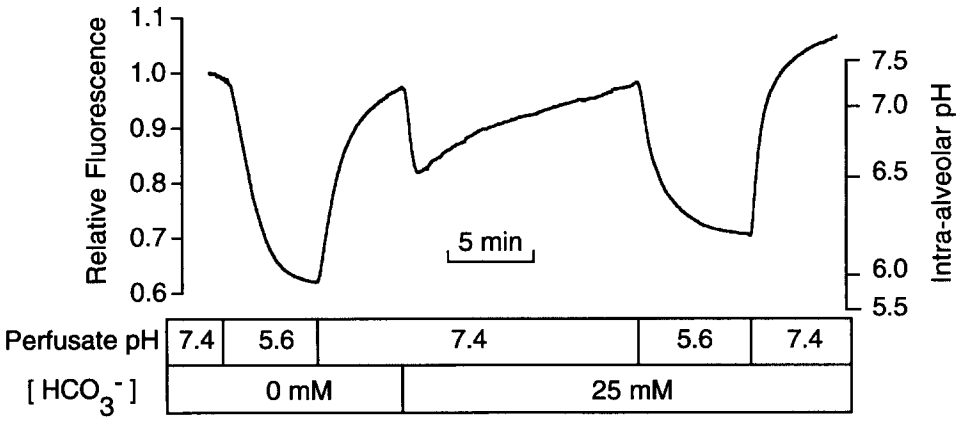

FIGURE 7. Proton transport measured in mouse lung by pleural surface fluorescence. The airspace was filled with HBR containing 1 mM FITC-dextran and the pulmonary artery was perfused with HBR at indicated pH or a HCO_3^--containing solution (see METHODS).

compartments, the surface fluorescence approach is technically simple and sensitive, and provides continuous information about intraalveolar fluid composition without the need to obtain samples from the distal airspace. In addition, unlike airspace fluid sampling methods, the surface fluorescence approach permits measurement of rapid transport processes in small animals.

The high permeability coefficient (P_f = 0.017 cm/s at 23°C) for osmotically driven water movement between the airspace and capillary compartments in mouse lung suggests the involvement of molecular water channels. For comparison, P_f is 0.0005–0.003 in the relatively water impermeable epithelium of thick ascending limb of Henle and the unstimulated kidney collecting duct (for review, see Finkelstein, 1989; Verkman, 1989). Examples of highly water permeable epithelia include the kidney proximal tubule (P_f 0.1–0.5 cm/s) and the vasopressin-stimulated collecting duct (0.02 cm/s). In a previous study in sheep lung, a lower limit for airspace-to-capillary P_f was estimated to be 0.01 cm/s at 20°C (Folkesson et al., 1994*b*), although this value had considerable uncertainty because the intratracheal installation time was comparable to the half-time for osmotic equilibration and because of difficulties in sampling airspace fluid. In the mouse lung here, osmotic water permeability was weakly temperature dependent and inhibited by $HgCl_2$, providing strong support for transalveolar water movement through molecular water channels.

The diffusional water permeability coefficient (P_d) in mouse lung was measured to be 1.3×10^{-5} at 23°C, giving an apparent P_f/P_d ratio of 1,300. In general, a P_f/P_d ratio of greater than unity is consistent with water passage through a pore-containing pathway (Finkelstein, 1989); however, an alternative explanation is that measured P_d underestimates true cell P_d because of the presence of unstirred layers. The unstirred layer can comprise barriers for water diffusion within cells, in the interstitium, and/or within the alveolus. Based on measurements in other water permeable epithelia such as the kidney proximal tubule and the vasopressin-stimulated collecting duct and amphibian urinary bladder (Levine et al., 1984; Verkman, 1989), a significant unstirred layer is predicted for transalveolar P_d, even if the interstitium and endothelial cell layer posed little resistance to water diffusion. Although the precise location of the unstirred layer barrier for P_d cannot be identified in this study, the high P_f/P_d compared with other tissues (P_f/P_d = 100, proximal tubule; 10–15, collecting duct; 17, toad bladder) suggests multiple barriers to water diffusion between the airspace and capillary compartments. It is noted that transepithelial osmotic water transport is relatively resistant to unstirred layer effects because of bulk water movement (Barry and Diamond, 1984). Unstirred layers for P_f arise from solute polarization near membrane surfaces due to convection-diffusion, rather than to simple diffusive barriers in the case of diffusional transport of water or solutes. The measured osmotic water permeability here is probably not much affected by unstirred layers based on the high P_f, low activation energy (E_a), and mercurial inhibition as well as the independence of P_f on osmotic gradient size and direction. Therefore, as found in several other epithelia, unstirred layers have a substantial effect on the determination of diffusional, but not osmotic water permeability.

A physiological role for lung water channels is suggested but not proven by the high airspace-to-capillary water permeability found here (for review of water channels, see Verkman et al., 1996; Agre and Nielsen, 1995). The AQP-1 (CHIP28) water channel is expressed primarily on alveolar capillary endothelia (Nielsen et al., 1993; Folkesson et al., 1994*b*; Hasegawa et al., 1994*a*) and to a lesser extent on type II alveolar epithelial cells (Folkesson et al, 1994*b*), which comprise a minority of alveolar surface area. The alveolar capillary endothelium probably poses a minor barrier to water and solute transport (Wangensteen, 1994). Furthermore, the normal phenotype of subjects lacking AQP-1 (Preston et al., 1994) suggests that AQP-1 is not re-

quired physiologically in lung. The mercurial-insensitive water channel (MIWC, AQP-4) (Hasegawa et al., 1994*b*; Yang et al., 1995, 1996) is primarily expressed at the basolateral membrane of airway epithelia (Frigeri et al., 1995), and probably facilitates *trans*-airway but not transalveolar water transport (Folkesson et al., 1996). A third water channel which is mercurial-sensitive (AQP-5) (Raina et al., 1995) is strongly expressed in lung and appears to be localized primarily to type I alveolar epithelia (unpublished results). The high transalveolar P_f measured here may thus be accounted for by AQP-5. In recent studies, expression of the three water channels in lung was found to be strongly increased just after birth (Umenishi et al., 1996). Direct evidence for a role of molecular water channels in lung function will require studies in transgenic knock-out mice or the development of nontoxic and selective water channel inhibitors.

There are several technical concerns in the application of the surface fluorescence method to measure airspace-capillary permeabilities. Potential serial permeability barriers exist between the capillary and airspace compartments, including capillary endothelial cells, the interstitium, alveolar epithelial cells, and aqueous-space unstirred layers. In general, the alveolar epithelium is believed to represent the major barrier to transport of small solutes (Wangensteen, 1994). The prompt fluorescence signal increase found here upon a change in perfusate fluid composition (Fig. 3 *A*) is consistent with the alveolar epithelium comprising the primary permeability barrier; a lag phase might be observed if the interstitium or endothelium pose a significant barrier to osmosis. In any epithelium, unstirred layers might influence apparent transport rates for solutes having high permeabilities, as was found here for diffusional water transport. Another concern in the interpretation of results is heterogeneity in alveolar size and transport properties. The experiments were carried out using a photomultiplier to integrate the signal arising from many individual alveoli and thus gave averaged permeability values. Alternatively, image analysis can be used to quantify permeability properties of many individual alveoli at the same time or to visualize a large area of lung surface to study regional heterogeneity. In addition, although no data are available, possible differences in transport properties of surface vs. deep alveoli should be considered. Finally, it is important to recognize that changes in the fluorescence of an intraalveolar indicator may arise both from changes in indicator concentration, resulting from osmotic water movement, as well as changes in indicator quantum yield resulting from specific indicator-solute interactions.

Notwithstanding these concerns, the surface fluorescence approach described here should have numerous applications in the quantitative measurement of water, solute, and ion transport in ex vivo and in vivo lungs. Transport of ions such as Cl^-, Na^+, and K^+ are measurable using suitable membrane-impermeant fluorescent indicators in the airspace (Verkman, 1995). Transport studies can be performed in lungs from small or large animals, provided that the airspace can be filled with saline containing appropriate fluorescent indicators. Our method should be particularly useful for transport measurements in control vs. transgenic mice and for studies of spontaneous fluid transport in intact lung under physiological conditions.

We thank Drs. Michael Gropper and Hans Folkesson for help with the initial surface fluorescence studies in rat lung.

This study was supported by National Institutes of Health grants HL51854, DK35124, HL42368, and DK43840, and grant R613 from the National Cystic Fibrosis Foundation. Mr. Farinas was supported by a fellowship from the American Heart Association, California Affiliate, and Dr. Carter was supported by a fellowship from the American Lung Association.

Original version received 12 April 1996 and accepted version received 22 May 1996.

REFERENCES

Acevedo, J.C., and E.D. Robin. 1972. Effect of intrapulmonary water instillation on pulmonary lymph flow and composition. *Am. J. Physiol.* 223:1433–1437.

Agre, P., and S. Nielsen. 1995. The aquaporin family of water channels in kidney. *Kidney Int.* 24:1057–1068.

Barry, P.H., and J.M. Diamond. 1984. Effects of unstirred layers on membrane phenomena. *Physiol. Rev.* 64:763–872.

Basset, G., C. Crone, and G. Saumon. 1987. Significance of active ion transport in transalveolar water absorption: a study on isolated rat lung. *J. Physiol. (Lond.).* 384:311–324.

Boucher, R.C. 1994. Human airway ion transport. Part one. *Am. J. Respir. Crit. Care Med.* 150:271–281.

Crapo, J.D. 1986. Morphologic changes in pulmonary oxygen toxicity. *Annu. Rev. Physiol.* 48:721–731.

Effros, R.M., G.R. Mason, J. Hukkanen, and P. Silverman. 1989. New evidence for active sodium transport from fluid-filled rat lungs. *J. Appl. Physiol.* 66:906–919.

Farinas, J., V. Simenak, and A.S. Verkman. 1995. Cell volume measured in adherent cells by total internal reflection microfluorimetry: application to permeability in cells transfected with water channel homologs. *Biophys. J.* 68:1613–1620.

Finkelstein, A. 1987. Water Movement through Lipid Bilayers, Pores, and Plasma Membranes: Theory and Reality. John Wiley & Sons Inc., New York.

Folkesson, H.G., F. Kheradmand, and M.A. Matthay. 1994*a*. The effect of salt water on alveolar epithelial barrier function. *Am. J. Respir. Crit. Care Med.* 150:1555–1563.

Folkesson, H., M. Matthay, A. Frigeri, and A.S. Verkman. 1996.

High transepithelial water permeability in microperfused distal airways: evidence for channel-mediated water transport. *J. Clin. Invest.* 97:664–671.

Folkesson, H.G., M.A. Matthay, H. Hasegawa, F. Kheradmand, and A.S. Verkman. 1994*b*. Transcellular water transport in lung alveolar epithelium through mercury-sensitive water channels. *Proc. Natl. Acad. Sci. USA.* 91:4970–4974.

Folkesson, H.G., M.A., Matthay, C.A. Hébert, and V.C. Broaddus. 1995. Acid aspiration–induced lung injury in rabbits is mediated by interleukin-8 dependent mechanisms. *J. Clin. Invest.* 96:107–116.

Frank, L., J.R. Bucher, and R.J. Roberts. 1978. Oxygen toxicity in neonatal and adult animals of various species. *J. Appl. Physiol.* 45: 699–704.

Frigeri, A., M. Gropper, C.W. Turck, and A.S. Verkman. 1995. Immunolocalization of the mercurial-insensitive water channel and glycerol intrinsic protein in epithelial cell plasma membranes. *Proc. Natl. Acad. Sci. USA.* 92:4328–4331.

Goodman, B.E., K.J. Kim, and E.D. Crandall. 1987. Evidence for active sodium transport across alveolar epithelium of isolated rat lung. *J. Appl. Physiol.* 62:2460–2466.

Hasegawa, H., S.C. Lian, W.E. Finkbeiner, and A.S. Verkman. 1994*a*. Extrarenal tissue distribution of CHIP28 water channels by *in situ* hybridization and antibody staining. *Am. J. Physiol.* 266: C893–C903.

Hasegawa, H., T. Ma, W. Skach, M.A. Matthay, and A.S. Verkman. 1994*b*. Molecular cloning of a mercurial-insensitive water channel expressed in selected water-transporting tissues. *J. Biol. Chem.* 269:5497–5500.

Kuwahara, M., and A.S. Verkman. 1988. Direct fluorescence measurement of diffusional water permeability in the vasopressin-sensitive kidney collecting tubule. *Biophys. J.* 54:587–593.

Levine, S.D., M. Jacoby, and A. Finkelstein. 1984. The water permeability of toad urinary bladder: II. The value of $P_f/P_d(w)$ for the antidiuretic hormone-induced water permeability pathway. *J. Gen. Physiol.* 83:43–61.

Matthay, M.A., H. Folkesson, and A.S. Verkman. 1996. Salt and water transport across alveolar and distal airway epithelia in the adult lung. *Am. J. Physiol.* 270:L487–L503.

Milsom, W.K. 1989. Comparative aspects of vertebrate pulmonary mechanics. *In* Comparative Pulmonary Physiology: Current Concepts, Vol. 39. S.C. Wood, editor. Marcel Dekker, Inc., New York. 587–619.

Nielsen, S., B.L. Smith, E.I. Christensen, and P. Agre. 1993. Distribution of the aquaporin CHIP in secretory and resorptive epithelia and capillary endothelia. *Proc. Natl. Acad. Sci. USA.* 90:7275–7279.

Olver, R.E. 1994. Fluid secretion and absorption in the fetus. *In* Fluid and Solute Transport in the Airspaces of the Lung. R.M. Effros and H.K. Chang, editors. Marcel Dekker, Inc., New York. 281–302.

Preston, G.M., T.P. Carroll, W.B. Guggino, and P. Agre. 1992. Appearance of water channels in *Xenopus* oocytes expressing red cell CHIP28 protein. *Science (Wash. DC).* 256:385–387.

Preston, G.M., B.L. Smith, M.L. Zeidel, J.J. Moulds, and P. Agre. 1994. Mutations in aquaporin-1 in phenotypically normal humans without functional CHIP water channels. *Science (Wash. DC).* 265:1585–1587.

Raina, S., G.M. Preston, W.B. Guggino, and P. Agre. 1995. Molecular cloning and characterization of an aquaporin cDNA from salivary, lacrimal, and respiratory tissues. *J. Biol. Chem.* 270:1908–1912.

Saumon. G., and G. Basset. 1993. Electrolyte and fluid transport across the mature alveolar epithelium. *J. Appl. Physiol.* 74:1–15.

Umenishi, F., E.P. Carter, B. Yang, B. Olivier, M.A. Matthay, and A.S. Verkman. 1996. Sharp increase in rat lung water channel expression in the perinatal period. *Am. J. Resp. Cell Mol. Biol.* In press.

Van Hoek, A.N., and A.S. Verkman. 1992. Functional reconstitution of the isolated erythrocyte water channel CHIP28. *J. Biol. Chem.* 267:18267–18269.

Verkman, A.S. 1987. Passive H^+/OH^- permeability in epithelial brush border membranes. *J. Bioenerg. Biomembr.* 19:481–493.

Verkman, A.S. 1989. Mechanisms and regulation of water permeability in renal epithelia. *Am. J. Physiol.* 257:C837–C850.

Verkman, A.S. 1995. Optical methods to measure membrane transport processes. *J. Membr. Biol.* 148:99–110.

Verkman, A.S., A.N. van Hoek, T. Ma, A. Frigeri, W.R. Skach, A. Mitra, B.K. Tamarappoo, and J. Farinas. 1996. Water transport across mammalian cell membranes. *Am. J. Physiol.* 270:C12–C30.

Wangensteen, O.D. 1994. Nonselective solute transport across the pulmonary epithelium. *In* Fluid and Solute Transport in the Airspaces of the Lungs, Vol. 79. R.M. Effros and H.K. Chang, editors. Marcel Dekker, Inc., New York. 374–397.

Weibel, E.R. 1989. Lung morphometry and models in respiratory physiology. *In* Respiratory Physiology. H.K. Chang and M. Paiva, editors. Marcel Dekker Inc., New York. 1–56.

Yang, B., D. Brown, and A.S. Verkman. 1996. The mercurial-insensitive water channel (AQP-4) forms orthogonal arrays in stably transfected CHO cells. *J. Biol. Chem.* 271:4577–4580.

Yang, B., T. Ma, and A.S. Verkman. 1995. cDNA cloning, gene organization and chromosomal localization of a human mercurial-insensitive water channel: evidence for distinct transcriptional units. *J. Biol. Chem.* 270:22907–22913.

Zen, K., J. Biwersi, N. Periasanny, and A.S. Verkman. 1992. Second messengers regulate endosomal acidification in Swiss 3T3 fibroblasts. *J. Cell Biol.* 119:99–110.